V European Conference on Computational Fluid Dynamics
ECCOMAS CFD 2010
J. C. F. Pereira and A. Sequeira (Eds)
Lisbon, Portugal,14-17 June 2010

A NUMERICAL STUDY OF THE FLOW IN A CYCLONE SEPARATOR USING THE $K-\epsilon$ REALIZABLE TURBULENCE MODEL

Mauricio Carmona*, Cristóbal Cortés† and Antonio Ramirez††

Center of research of Energy Resources and Consumptions (CIRCE),
Department of Mechanical Engineering, University of Zaragoza
María de Luna 3, 50018 Zaragoza, Spain
*e-mail: mcarmona@unizar.es †e-mail: tdyfqdb@unizar.es ††e-mail: jaramvaz@unizar.es

Key words: Computational Fluid Dynamics, Cyclone, URANS, $k-\epsilon$ realizable, Grid Convergence Index

Abstract. *Numerical simulation of a cyclone separator with the Unsteady, Reynolds-Averaged Navier-Stokes (URANS) equations is presented. The $k-\epsilon$ realizable turbulence model is chosen as the closure model in view to its reduced computational expense as compared to the Reynolds Stress Model (RSM). Since the model is still relatively new, it has not been demonstrated under which conditions this model presents good approximations, and there is no bibliographical reference of any study of application of this model to the simulations of cyclones. Results show that the $k-\epsilon$ realizable turbulence model is capable of reproducing the oscillating and non-axisymmetric behavior of the flow structure in cyclones.*

A Grid Convergence Index (GCI) study is carried out using three systematically structured meshes in order to corroborate that the time-averaged and temporal results are reproduced with grid resolution independence. Spectral analysis and coherent structures are documented by means of fast Fourier transform (FFT) and visualization techniques.

1 INTRODUCTION

Cyclone separators are devices widely used in the industry. Several features such as their simple and compact design, low cost and almost maintenance-free operation, no moving parts involved, flexibility of manufacture materials, good performance in extreme conditions like high temperatures, pressures, and corrosive atmospheres, explain their popularity in separation processes and product recovery.

In spite of the great development of the Computational Fluid Dynamics (CFD) simulations, the use of experimental traditional methods has prevailed over the numerical in the design and study of cyclones. This is because the inner flow in these devices entails high complexity; it's a three-dimensional flow with high intensity of rotation in which coherent structures dependent of the time appear[1]. The simple turbulence models widely used as the standard and RNG $k-\epsilon$ are not able to predict these complex conditions, so that this demands the use of models more expensive in terms of computing resources.[1−9]

On the other hand, the traditional semi-empirical models have given acceptable results for the requirements in the design, which has limited the range of applications of CFD for cyclone devices. Nevertheless, the empirical models suffer the deficiency that they can only be used within the experimental limits from which the parameters were determined. For this reason, the analysis in the geometric modifications or other parameters of design in experimental form are more difficult to perform. Additionally, to detect the complex behavior in the flow inside cyclones is difficult with the current measurement techniques. Recently the CFD models appear as a less expensive alternative to study these complex flows than the experimental techniques. However, to reproduce this behavior in a numerical model is not an easy task. Significant advances have been accomplished in the use of CFD for cyclone applications in the last decades. Revisions of the early experimental works and simulations of cyclones and hydrocyclones are shown in references [1, 3, 5, 6, 9−11].

Simulations with the $k-\epsilon$ standard turbulence model have demonstrated that it doesn't have the capacity to predict the complex features of the inner flow in cyclones separators.[2−4,10,11] Morever, in order to improve the predictions, some authors[2−4,10−13] have used modified models as the $k-\epsilon$ Renormalization Group (RNG), obtaining poor results. The general conclusions show that is necessary the use of the Reynolds Stress Model (RSM)[1−14] or superior models as LES[1,5,12] to obtain good results for numerical simulation of cyclones separators. Although these advanced models are capable to predict the complex behavior in the inner flow of a cyclone, are more expensive in computational time than that $k-\epsilon$ model, which makes them impractical in the design and optimization process in this device.

The $k-\epsilon$ realizable turbulence model is still relatively new and it is not clear in exactly which instances the model presents good performance, and there is no bibliographical reference of any study of application of this model in cyclone simulations. In order to find a simulation methodology in cyclones separators that present good performance with a

reasonable computer cost, in this work a numerical simulation process of a cyclone with a $k-\epsilon$ realizable turbulence model is accomplished. Solid particles were not considered in this study; therefore, only the air flow was taking into account so that describe the flow field. A Grid Convergence Index (GCI) was carried out with three systematically structured meshes, using the commercial Software FLUENT 6.3.26 for transient state. As it will be show below, this model is capable of reproducing the oscillatory and non-axisymmetric behavior of the flow structure in cyclones separators.

2 MODEL DESCRIPTION

2.1 Cyclone geometry

Regardless of the complexity of the inner flow in a cyclone, its basic principle of operation and geometry are simple. The cyclone investigated is based on the work reported in [2]. This device uses a prolonged cylindrical tube located at the bottom of the main body denominated "dipleg" as a mechanism to collect the solids. The main dimensions of the body and dipleg of the cyclone are shown in figure 1.

The solid particle extraction in the cyclone is made mean a suction nozzle located on the bottom of the dipleg, perpendicular to the cyclone axis. For the simulation this solid extraction is considered as an air outflow boundary condition, which was measured experimentally in [2] and [15]. The suction nozzle is simulated as a cylindrical duct with diameter 10 [mm] as shown in figure 1.

2.2 Boundary conditions

For this problem the boundary conditions are based on the experimental tests carried out by [2] and [15]. The inlet boundary condition is an inflow with a constant velocity of $v_i = 13.4[m/s]$, on the other hand the air mass flux reported at the extraction nozzle is $\dot{m}_{ext} = 0.000583[Kg/s]$ and the operation pressure is 322 [KPa]. Mass conservation then gives the air outflow.

The boundary conditions for the turbulence parameters on the inlet and exit regions were taken from the Reynolds number (Re_{D_h}), the hydraulic diameter (D_h) and turbulence intensity(I) terms.

In order to consider the wall effects and prevent the numerical solution in the near-wall region, the wall functions approach, which applies boundary conditions based on the logarithmic law relations in the adjacent nodes to the wall has been used.[16,17]

2.3 First node distance

To estimate the first node distance so that this element will be located within the log-law region, velocity estimations inside cyclones have been used, as done in the reference [1] and [2] for the Alexander, Barth y Meissner y Löffler models. The estimated values of tangential velocity by these models near to the wall of the cyclone body are in the range of 16.84 to 22.48 [m/s]. With these forecasts and using the recommended values

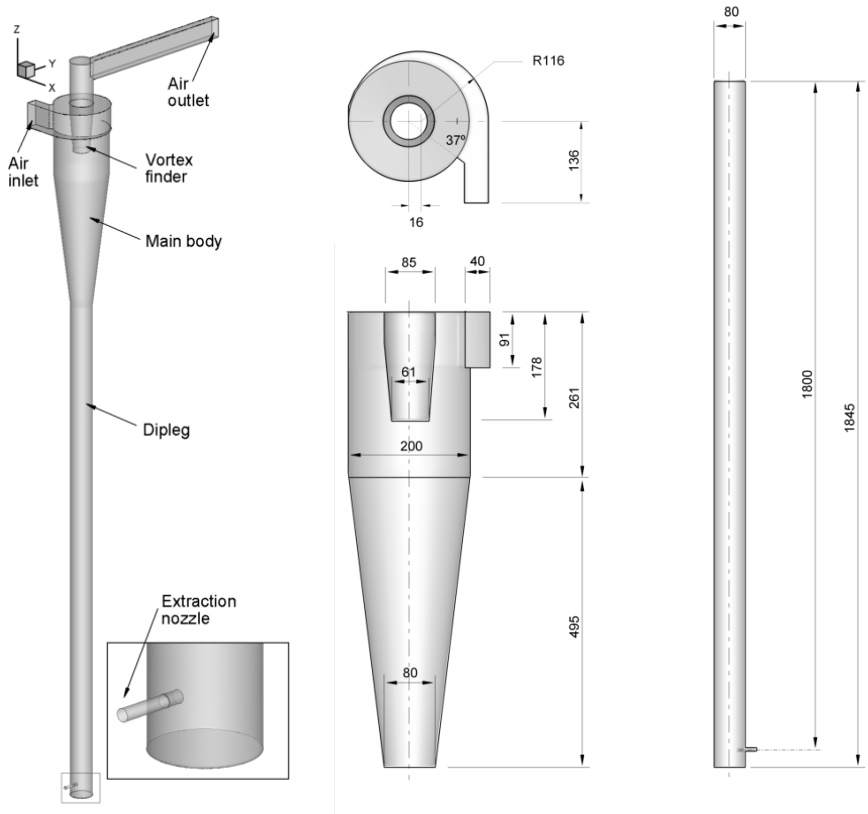

Figure 1: Parts and main dimensions of the body and dipleg of the cyclone (All measurement in [mm])[2]

for the dimensionless wall coordinate y^+ in [18], [16] and [17] for the logarithmic region, the range for the first node distance on the grid y_p is:

$$0.37[mm] < y_p < 10[mm] \tag{1}$$

2.4 Measurement points

Measurement lines on the cyclone body were taken arbitrarily for comparison purposes, in addition, measurement lines in the dipleg were used and are denoted from top to bottom as A, B, C, D, and F respectively. The locations of these lines are shown in figure 2. The data was taken from the wall to the cyclone axis obtaining a velocity profile for each measurement line.

For the mesh convergence study and the temporal analysis is necessary to take a record of the velocity evolution in different points throughout the simulations for the three grids. Five arbitrary points in the main cyclone body and two gauge points for each measurement lines (A -F) in the dipleg were taken for comparison purposes. The first point by each measurement line in the dipleg is denoted as a_1, b_1, ..., f_1 and are located on its respective measurement line to 33 [mm] from the dipleg axis; the second point for each measurement

line in the dipleg is denoted as a_2, b_2, ..., f_2 and are located on its respective measurement line to 21 [mm] from the dipleg axis. The location of the measurements points are shown graphically in figure 2, and the exact positions of the arbitrary points in the main cyclone body are shown in table 1, where D_C is the cyclone diameter and the origin of the coordinate system is located on the top of the cyclone body.

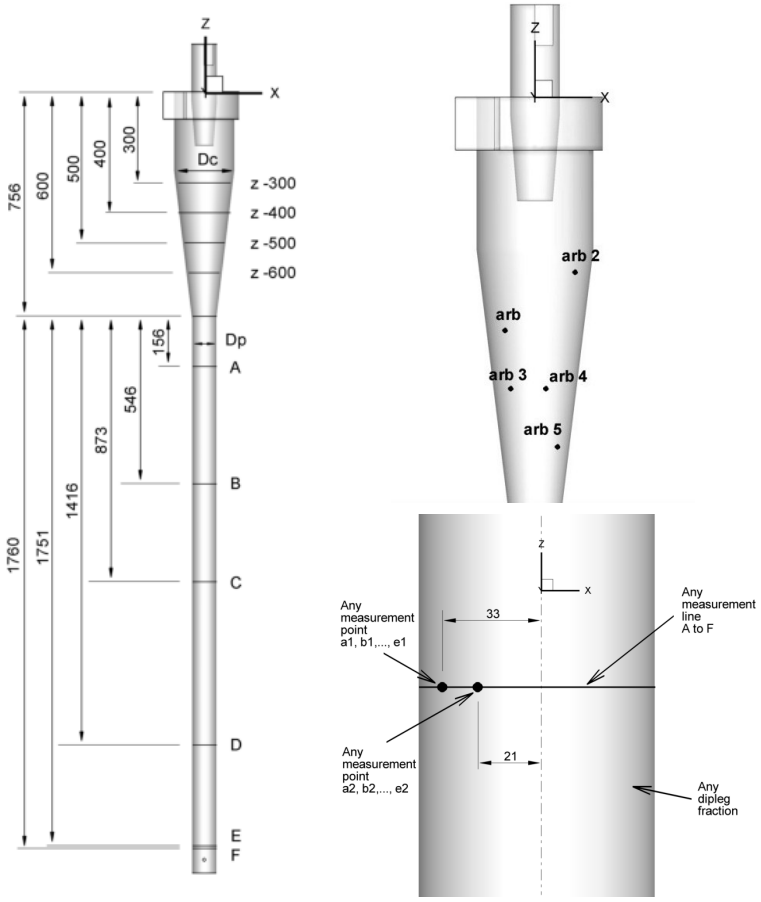

Figure 2: Graphical location of the measurement points (All measurement in [mm])

Measurement point	X/D_C	Y/D_C	Z/D_C
Point arb	-0.25	0	-2
Point arb 2	0.35	0	-1.5
Point arb 3	-0.2	0	-2.5
Point arb 4	0.1	0	-2.5
Point arb 5	0.2	0	-3

Table 1: Location of the arbitrary measurement points in the main cyclone body

3 SIMULATION MODEL

Computer simulations were carried out with the program Fluent version 6.3.26, using as preprocessor the program Gambit version 2.2.

3.1 Governing equations and turbulence model

The Unsteady, Reynolds Averaged Navier-Stokes (URANS) equations are solved for isothermal and incompressible flow for the single phase of air, adopting two different closures for turbulence, the standard $k-\epsilon$ model[21] and the realizable $k-\epsilon$ model[22].

3.2 Discretization error estimation

In order to corroborate that the solution is independent of the grid resolution, a study of grid convergence was made. With this study, the truncation error is reduced and the best degree of grid resolution is defined. This method consists in starting with an initial grid and then make consecutive refinements to observe the effect of the grid resolution.[19]

The recommended method for discretization error estimation is the Grid Convergence Index (GCI) based on the Richardson Extrapolation (RE) method, that involves comparisons between two different grid sizes.[20] This method is currently the most robust method available for the prediction of numerical uncertainty, in spite that it is far from being perfect. The GCI method shown good performance for numerous and different CFD cases.[19] In order to quantify the discretization error, the systematic procedure recommended by [19] was followed.

3.3 Meshing scheme

It is convenient that the meshing process is carried out in steeped form in order to guarantee the validity of the discretization error estimation method described above.[19] Taking into account the work of [2] as a base and considering the estimate range for the first node centroid [eq (1)], three structures and stepped grids were made (coarse, medium, fine). Adjacent elements to the wall are in the logarithmic region, guaranteeing the correct application of the wall functions.

In the cylindrical zones like the cyclone body, the vortex finder and the cyclone dipleg, and in rectangular regions like the gas inlet and gas outlet section a structural meshing with hexahedral elements was done. On the other hand in zones with geometries with high complexity like the scroll and the air extraction nozzle at the bottom of the dipleg, an unstructured meshing with tetrahedral elements was used.

The target value for the grid refinement factor $r = h_{coarse}/h_{fine}$ is 2. Nevertheless, in practice this is not possible due to the unstructured mesh zones. The numbers of computational cells for the geometry are 4 058 322, 1 450 742 and 570 016 for the fine, medium and coarse grids respectively. The refinement factors $r_{21} = h_{medium}/h_{fine}$ and $r_{32} = h_{coarse}/h_{medium}$ are 1.409 and 1.365 respectively. Therefore, $r = 1.923$. This value is in the range recommended by [20].

Details of the computational mesh are shown in figure 3.

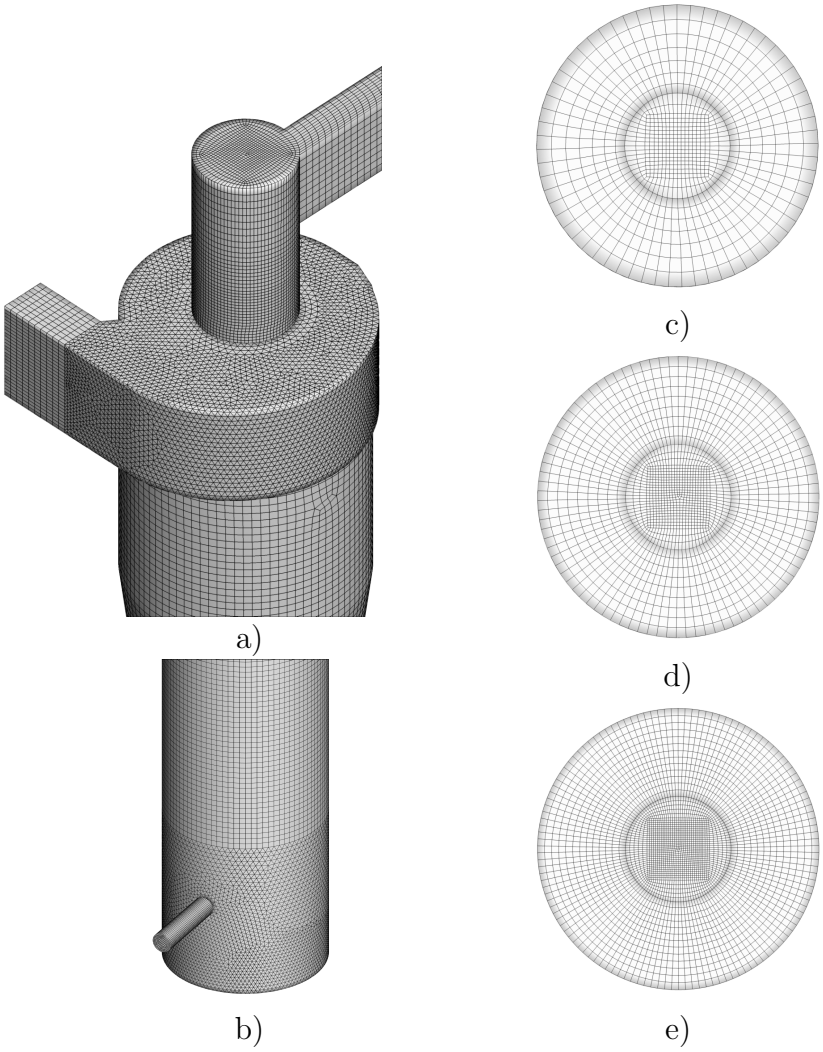

Figure 3: Details of the computational mesh: a) Cyclone body. b) Details of extraction nozzle. Grid refinement: c) coarse, d) medium and e) fine

3.4 Simulation process

In this case the convergence in the simulations can be difficult to reach; therefore to have an initial solution, it is necessary to start from a simple turbulence model as a first step, the $k-\epsilon$ standard turbulence model was used with four orders of magnitude decrease in the normalized residuals for each equation solved. The resulting flow is not correct but provides an initial solution in the use of most advanced turbulence models. As concluded by several bibliographic references [2−4, 10, 11], the $k-\epsilon$ standard turbulence

model doesn't have the capability to predict the complex periodical and three-dimensional features innate in this kind of device. In own conditions the solution reached the steady state convergence.

This solution was used as the base for the simulations with the $k-\epsilon$ realizable turbulence model. For Pressure-Velocity coupling the SIMPLE algorithm was used, the Second Order Upwind scheme was applied for spatial discretization, finally the pressure interpolation scheme adopted was the PRESTO! (PREssure STaggering Option) scheme, which is the recommended scheme in order to improve the estimation for highly swirling flows simulations.[16] The residuals exhibit cyclic tendencies at these conditions, which is an indicator that a transient pattern occurs. For cyclone applications this kind of tendencies are obtained when advanced turbulences models like the RSM are used.[23] At this point the simulations were carried out in transient state, the iterative convergence at each time step was verified.

Taken into account the report of [2], which showed that the periodic flow estimated by the simulations in this cyclone presented an oscillation frequency in the order of 100 [Hz], to observe the numerical effects in the time step selection, simulations with four values of time step (0.001, 0.0005, 0.0001 and 0.00005 [s]) were carried out. Only the last two values of time step predicted both, the average values and fluctuations with the same results. To reduce the simulation computer time, a time step of 0.0001 [s] was chosen. For this condition an oscillatory solution was obtained in a reduced number of iterations in all control points. The coarse, medium and fine grids exhibit the same behavior in the simulations.

4 RESULTS AND DISCUSSION

4.1 Averaged velocities and Grid Convergence Index (GCI)

In the left side of figure 4 the averaged axial and tangential velocities profiles for the coarse, medium and fine grids are shown as an example, while in the right side it shows both, the averaged axial and tangential velocities profiles with their corresponding discretization error estimation in form of error bars for the medium grid at the measurement line A of the dipleg. For the vertical axis in this figure, the obtained velocity in the simulation was divided by the inlet velocity $V_e = 13.4m/s$, whereas the horizontal axis is X/R_c, where X is the measure in the point and $R_c = D_c/2 = 0.1[m]$ is the cyclone radius. With these variables $X/R_c = 0$ is the cyclone - dipleg axes. The measurement lines B to F have the same behavior as the A line, but are not shown for brevity.

On the other hand, figure 5 shows the same information that figure 4 for the measurement line $z-600$ of the cyclone body. Again the measurement lines $z-300$ to $z-500$ have the same behavior as the $z-600$ line, but are not shown for brevity.

The three grids used with the GCI method show that the apparent order of accuracy p ranges from 0.23 to 8.8, with an average of 3.73 in the measurements lines on the cyclone dipleg (A-F) for the velocity magnitude. The maximum discretization uncertainty is 22.6%

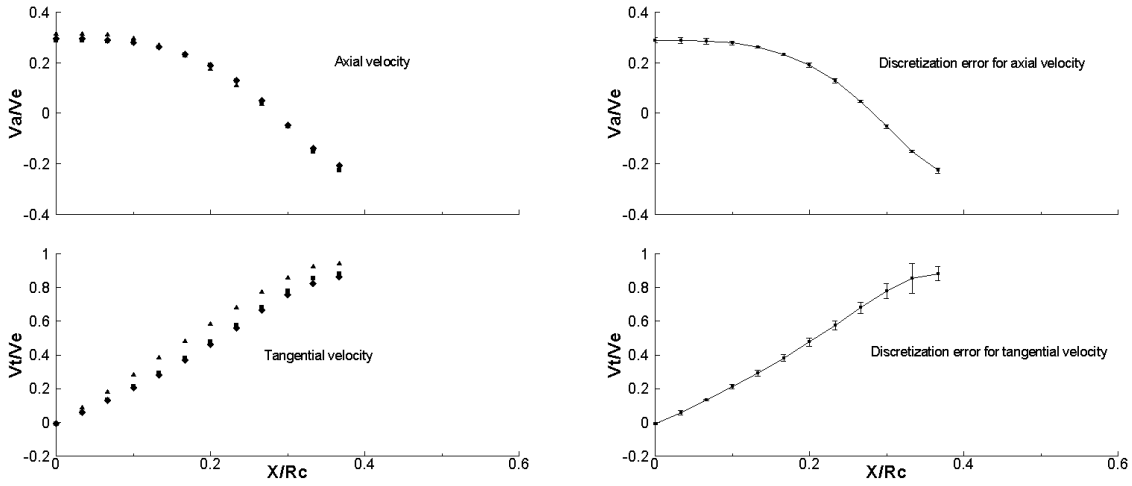

Figure 4: Averaged axial and tangential velocities: Profiles for the coarse (⧫), medium (■) and fine (▲) grids (Left) Discretization error for the medium grid (Right); measurement line of the dipleg A

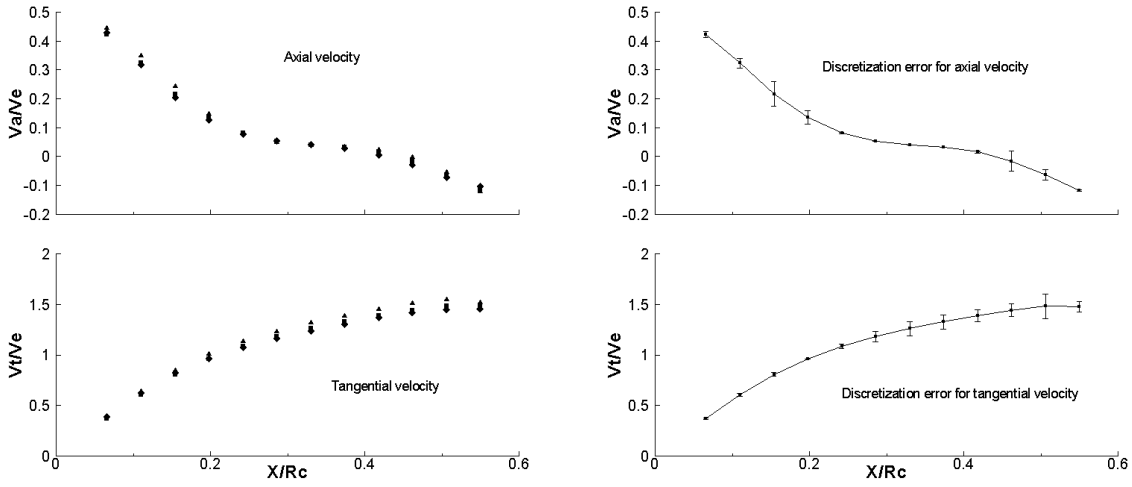

Figure 5: Averaged axial and tangential velocities: Profiles for coarse (⧫), medium (■) and fine (▲) grids (Left) Discretization error for the medium grid (Right); measurement line of the cyclone body $z - 600$

with an average of 8.8%. Oscillatory convergence occurs at 26.7% of total measurement points in the cyclone dipleg. Additionally, in the measurement lines in the cyclone body, the apparent order of accuracy p ranges from 1.1 to 10.23, with an average of 2.33 for the case of the velocity magnitude. The maximum discretization uncertainty is 11.8% with an average of 4.2%. Oscillatory convergence occurs at 8.33% of total measurement points in the cyclone body.

The difference between the three grids results is negligible in each measurement point for the averaged axial and tangential velocities in the body and dipleg of the cyclone. For

the GCI method, the error intervals are small, therefore the estimation of the medium grid in the body and dipleg of the cyclone is numerically accurate in terms of the averaged solution.

4.2 Flow behavior

In order to detect special features in the flow inside of the cyclone, figure 6 shows the iso-surface of zero axial velocity inside cyclone, for different simulation times. This surface separates the upward and downward vortex flows and as shown in the figure, it has a non-axisymmetric shape which changes over time.

Figure 7 shows a field of axial velocity in cross-sectional plane $z - 600$ showed in figure 2 at different simulation times.

Figures 6 and 7 shows that the closure model used have the capability to predict the oscillatory and three dimensional behavior innate in this kind of devices.

4.3 Spectral analysis

The Fast Fourier Transform (FFT) was applied to the time evolution of the axial and tangential velocities in the measurements points in the body and dipleg of the cyclone in order to compare the estimated frequency content. In the left side of figure 8 the axial and tangential velocities throughout the simulations for the measurement point a_1 located at the cyclone dipleg for the coarse, medium and fine grids are shown as an example, whereas in the right side it shows the FFT of these records for the same measurement point. Analogously figure 9 also shows the same information as other example for the measurement point *arb* 5 located at the cyclone body. In the FFT graphics the vertical axis is the magnitude of the velocity in $[m/s]$, while the horizontal axis is the frequency in $[Hz]$. Other measurement points at the dipleg and the body of the cyclone, exhibit a similar behavior.

The temporal signals are slightly out of phase; however the simulations for the medium and fine grids have equivalent ranges, the FFT for all measurement points show similar behavior for all the grids.

With this observations it is possible conclude that the estimate dominant frequency values of oscillation and velocities magnitudes for the inlet flow in the cyclone agree for the medium and fine grids, therefore, convergence solution in the transitory simulations for the medium grid was reached.

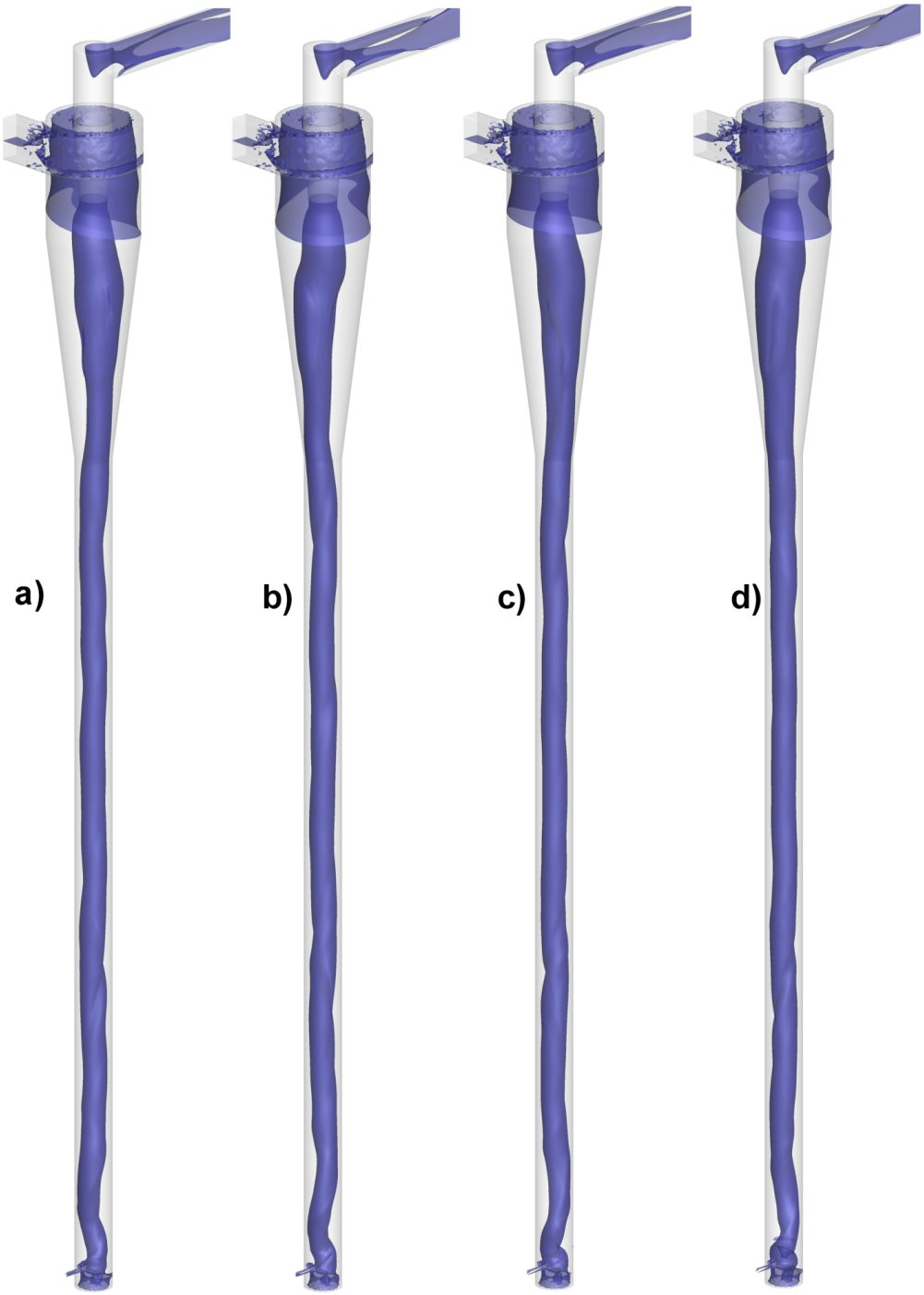

Figure 6: Iso-surface of zero axial velocity inside cyclone for different times: a) $t = 12.72[s]$; b) $t = 12.76[s]$; c) $t = 12.80[s]$; d) $t = 12.84[s]$

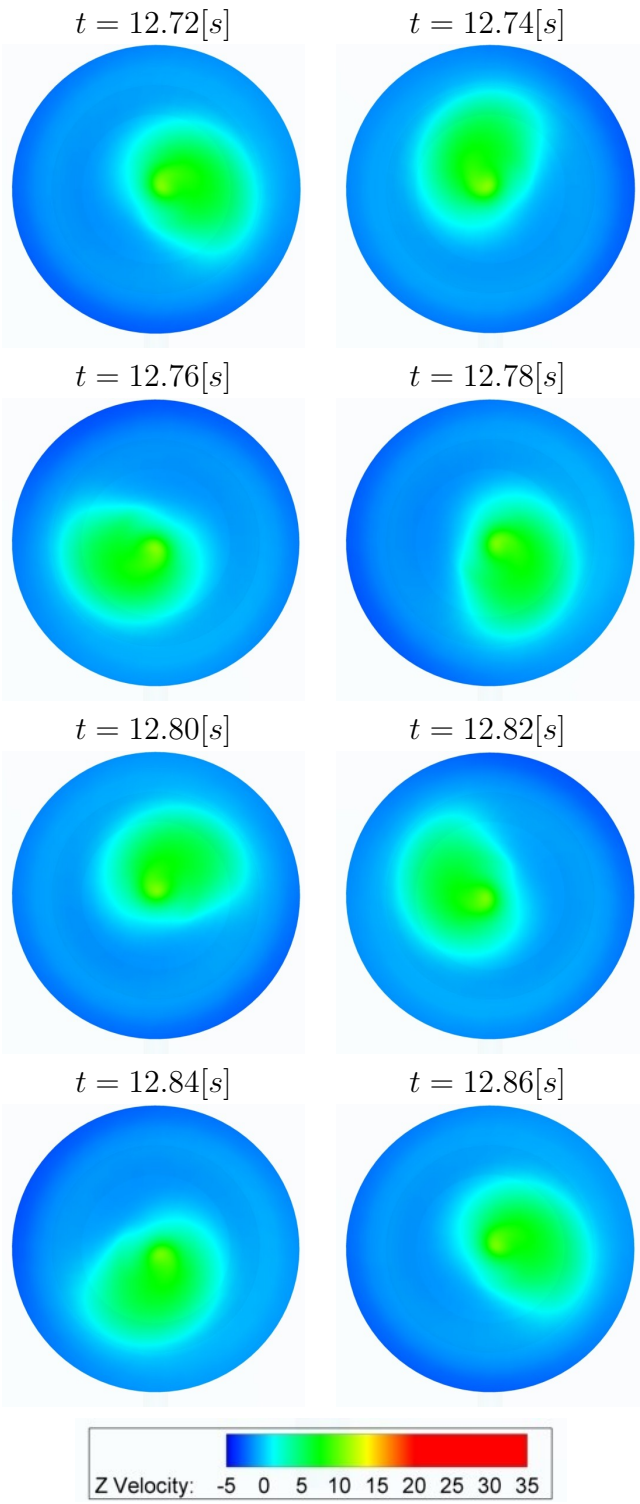

Figure 7: Field of axial velocity at different simulation times, cross-sectional plane: $Z = -0.6[m]$

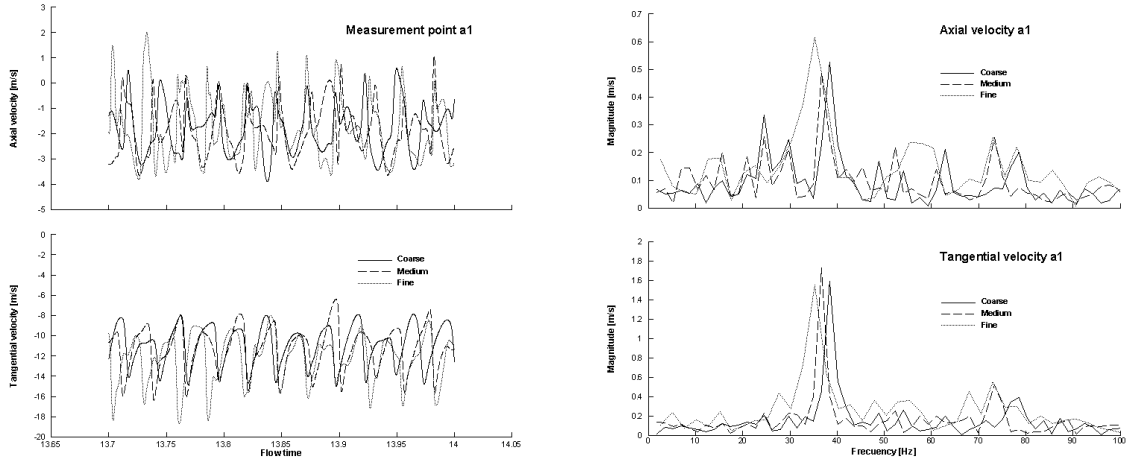

Figure 8: Axial and tangential velocities records (Left) and FFT (Right) for the coarse, medium and fine grids in the measurement point at the cyclone dipleg a_1

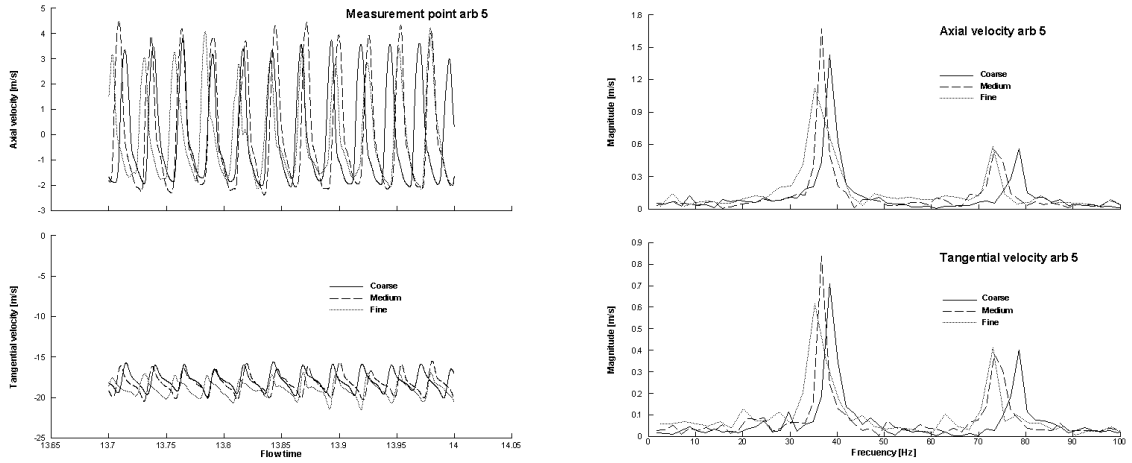

Figure 9: Axial and tangential velocities records (Left) and FFT (Right) for the coarse, medium and fine grids in the measurement point at the cyclone body *arb* 5

5 CONCLUSIONS

- In this work a numerical simulation of a cyclone separator was presented using the CFD commercial software Fluent 6.3.26. Grid Convergence Index (GCI) was showed for the axial and tangential velocities results with three systematically structured and stepped meshes. The simulations started from a simple stationary case with the $k-\epsilon$ standard turbulence model with a scheme of first order discretization, until it reached oscillating convergence for transitory state with the $k-\epsilon$ realizable turbulence model with a scheme of second order discretization.
- Results of the simulation show that the velocity in the near-wall region for the cyclone

body agreed with initial velocity estimate, guaranteeing the correct application of the wall functions.

- The $k-\epsilon$ standard turbulence model was not enough to predict the complex periodical and three-dimensional features innate in inner flow of cyclone separators.
- The difference for the averaged axial and tangential velocities in the body and dipleg of the cyclone is negligible. On the other hand, the orders in the dominant frequencies and velocities magnitudes in the FFT agree for the estimations of the three grids. Then, the medium grid has reached a convergence value in the transitory simulations.
- Finally the $k-\epsilon$ realizable turbulence model was shown to have the capability of reproducing this kind of complex flows, reaching transitory oscillatory solutions. This conclusion is presented on several bibliographic references only when more advanced and expensive computationally turbulence model are employed.

REFERENCES

[1] Cristóbal Cortés and Antonia Gil, Modeling the gas and particle flow inside cyclone separators, *Progress in Energy and Combustion Science, ELSEVIER*, **33** 409-452 (2007)

[2] José Velilla, Estudio el flujo en el interior del conducto de extraccin de slidos de un cicln de una central trmica de lecho fluido a presin, *Tesis Doctoral Universidad de Zaragoza* , (2004)

[3] W. D. Griffiths and F. Boysan, Computational Fluid Dynamics (CFD) and empirical modelling of the performance of a number of cyclone samplers, *J. Aerosol Sci. ELSEVIER*, **Vol. 27, No. 2** pp. 281-304 (1996)

[4] T.G. Chuah, Jolius Gimbun, Thomas S.Y. Choong, A CFD study of the effect of cone dimensions on sampling aerocyclones performance and hydrodynamics, *Powder Technology, ELSEVIER*, **162** 126 - 132 (2006)

[5] M. Narasimha, Mathew Brennan, P.N. Holtham, Prediction of magnetite segregation in dense medium cyclone using computational fluid dynamics technique, *Progress in Energy and Combustion Science, ELSEVIER*, **33** 409-452 (2007)

[6] S. Schuetz, G. Mayer, M. Bierdel, M. Piesche, Investigations on the flow and separation behaviour of hydrocyclones using computational fluid dynamics, *Int. J. Miner. Process, ELSEVIER*, **73** 229- 237 (2004)

[7] Gujun Wan, Guogang Sun, Xiaohu Xue, Mingxian Shi, Solids concentration simulation of different size particles in a cyclone separator, *Powder Technology, ELSEVIER*, **183** 94-104 (2008)

[8] Luiz G.M. Vieira, Carlos A. Silva Jr., Joao J.R. Damasceno, Marcos A.S. Barrozo, A study of the fluid dynamic behaviour of filtering hydrocyclones, *Separation and Purification Technology, ELSEVIER*, **58** 282-287 (2007)

[9] Steffen Schütz, Gabriele Gorbach, Manfred Piesche, Modeling fluid behavior and droplet interactions during liquid- liquid separation in hydrocyclones, *Chemical Engineering Science, ELSEVIER*, **54** 2055-2065 (1999)

[10] K. Udaya Bhaskar, Y. Rama Murthy, M. Ravi Raju, Sumit Tiwari, J.K. Srivastava, N. Ramakrishnan , CFD simulation and experimental validation studies on hydrocyclone, *Minerals Engineering, ELSEVIER*, **20** 60-71 (2007)

[11] A.J. Hoekstra, J.J. Derksen, H.E.A. Van Den Akker, An experimental and numerical study of turbulent swirling flow in gas cyclones, *Chemical Engineering Science, ELSEVIER*, **54** 2055-2065 (1999)

[12] Jose A. Delgadillo, Raj K. Rajamani, A comparative study of three turbulence-closure models for the hydrocyclone problem, *Int. J. Miner. Process, ELSEVIER*, **77** 217- 230 (2005)

[13] Jin W. Lee, Hoe J. Yang, Dong Y. Lee, Effect of the cylinder shape of a long-coned cyclone on the stable flow-field establishment, *Powder Technology, ELSEVIER*, **165** 30-38 (2006)

[14] Arman Raoufi, Mehrzad Shams, Meisam Farzaneh, Reza Ebrahimi, Numerical simulation and optimization of fluid flow in cyclone vortex finder, *Chemical Engineering and Processing, ELSEVIER*, **46** 128-137 (2008)

[15] Antonia Gil, Modelo experimental de flujo frío del ciclón primario de una planta de lecho fluido a presión, *Tesis Doctoral Universidad de Zaragoza* , (2000)

[16] User's Guide, *Fluent documentation*, **Version 6.3.26**

[17] Stephen B. Pope ,Turbulent flows, *Cambridge* , (2000)

[18] Frank M. White, Viscous Fluid Flow, *McGraw-Hill* , **Second edition** (1991)

[19] Ismail B. Celik, Procedure for Estimation and Reporting of Discretization Error in CFD Applications, *Journal of Fluids Engineering, ASME*, **Vol 130/078001-1** (2008)

[20] P.J. Roache, Quantification of uncertainty in computational fluid dynamics, *Annual Reviews Inc. Fluid. Mech*, **29** 123-60 (1997)

[21] Launder, B. E. and Spalding, D. B, The numerical computation of turbulent flows, *Computer Methods in Applied Mechanics and Engineering*, **3(2)** 269-289 (1974)

[22] T.-H Shih, W. W. Lion, A. Shabbir, Z. Yang, and J. Zhu, A new $k - \epsilon$ Eddy Viscosity Model for High Reynolds Number Turbulent Flows-Model Development and Validation, *Computers Fluids*, **24(3)** 227-238 (1995)

[23] Jolius Gimbun, T.G. Chuah, A. Fakhru'l-Razi, Thomas S.Y. Choong, The influence of temperature and inlet velocity on cyclone pressure drop: a CFD study, *Chemical Engineering and Processing, ELSEVIER*, **44** 7-12 (2005)